FUOYE Journal of Engineering and Technology, Volume 9, Issue 4, December 2024 ISSN: 2579-0617 (Paper), 2579-0625 (Online)

Trends of Corrosion Rate Assessment in Hydrochloric Acid Reinforced Concrete Environment

*[1]Ilesanmi O. Olofintuyi, [2]Chinwuba Arum, [3]Samuel L. Akingbonmire and [4]Bolanle A. Ojokoh
[1]Department of Civil Engineering, Federal Polytechnic, Ado Ekiti, Nigeria
[2,,3]Department of Civil Engineering, Federal University of Technology, Akure, Nigeria
[4]Department of Computing, Federal University of Technology Akure, Nigeria
olofintuyi_io@fedpolyado.edu.ng, [2]arumcn4christ@yahoo.co.uk, [3]sakingbonmire@futa.edu.ng and [4]baojokoh@futa.edu.ng

Received: 04-SEPT-2024; Reviewed: 12-DEC-2024; Accepted: 23-DEC-2024
https://dx.doi.org/10.4314/fuoyejet.v9i4.19

ORIGINAL RESEARCH

Abstract— The purpose of this study was to evaluate how corrosion treatments affected the rates of corrosion in concrete technology. Concrete samples of 140 mm x 100 mm x 50 mm were reinforced with reinforcing materials (give the name of the material) , and corrosion was measured gravimetrically. Concrete samples were combined in a 1:2:4 ratio and exposed to 0.1M, 0.2M, and 0.3M of HCl acid, while distilled water served as the control. The findings demonstrated that, with the exception of 0.3M, corrosion rates reduced as the number of observation days rose. Over the course of seven days, the corrosion rates for 0.1M HCL, 0.2M HCl, and 0.3M HCl were 0.853mm/yr, 0.804mm/yr, and 0.153mm/yr respectively. Corrosion rates increased and decreased at 0.3M for 21 days after being similar for 14 days. Corrosion rates at 28 days were 0.057776 mm/yr, 0.068321 mm/yr, and 0.061989 mm/yr for concentration levels of 0.1M, 0.2M, and 0.3M, respectively. As HCl acid environment concentration levels increase, the research indicates that corrosion rates for reinforced concrete decrease with increasing observation ages. This could be because the acid progressively turns the concrete alkaline, forming a protective coating over the buried steel.

Keywords— Corrosion, corrosion rates, residual strength, sensor-enabled method, weightloss, Potentio-dynamic polarization test

◆

1 INTRODUCTION

When faced with construction jobs requiring technical competence, concrete has shown to be the only viable solution to the problems posed by nature and its surroundings [Kumar et al., (2013), Tachibana, et al., (1990), Nikitasari, et al., (2022)]. It is evident that in today's world, concrete has become the material of choice for building a vast array of different types of constructions. Because of this, concrete is used a lot in the current construction sector to build structures like bridges, culverts, beams, columns, and barriers. The history of building collapses in developing nations has demonstrated that concrete's compressive strength and service life are often overlooked by designers, who are more concerned with the immediate work at hand than with potential future problems. Al-Saidy *et al.*, (2009) discovered that each year, building owners and managers must bear the expense of fixing concrete that spalls when the reinforcing steel corrodes. This is typically caused by the presence of salt, which causes the reinforcement to corrode and lose its corresponding strength. However, the volume of rust products, such as ferric oxides or hydroxides, whose volume is three to six times greater than the volume of steel, also contributes to the problem [Kumar at al., (2013), Khavasfar, *et al.*, (2007), Patil, *et al.*, (2022)]. Even if the cover zone, or concrete cover, of concrete is disrupted, reinforcement corrosion is a key cause of degradation. [Al-Saidy *et al.*, (2009), Malaret, (2022) Fernandez, *et al.*, (2016)] discovered that the flexural strength capacity of concrete decreases in proportion to the corroding steel's loss of cross-sectional area. In actuality, the amount of steel that corrodes actually increases relative to the original steel since it does so gradually and applies a significant tensile force on the concrete, which shortens its service life by causing it to fracture and spall off.

In related research carried out by Cáceres, *et al.*, (2019) to comparatively study gravimetric and electrochemical techniques on the evaluation of corrosion inhibitor activity onset and efficiency in pipeline CO2 environments, they established that, the corrosion rates from linear polarization resistance in the solution without inhibitor were overestimated, while the Harmonic Distortion Analysis and enhanced Electrical Resistance presented similar results to Standard Coupon.

The Tafel plots and Polarization resistance curve are often affected by scan rate or charging current as discovered by Zhang *et al.*, (2006) they opined that, the extent of the distortion of the polarization curve can reflect the difference between the two potentials. Some significant errors are introduced into the values of the corrosion current density and Tafel slopes due to this distortion.

Corrosion of steel in reinforced structures cannot be separated, a large number of methods have been utilized to study corrosion rates of reinforced concrete structures/elements. According to a review by Song and Saraswathy, (2007) on “Corrosion Monitoring of Reinforced Concrete Structures” several corrosion monitoring mechanisms were discussed, it was resolved

---

*Corresponding Author:

Section E- CIVIL ENGINEERING AND RELATED SCIENCES
Can be cited as:
Olofintuyi I.O., Arum C., Akingbonmire S.L. and. Ojokoh B. A. (2024). Trends of Corrosion Rate Assessment in Hydrochloric Acid Reinforced Concrete Environment. In FUOYE Journal of Engineering and Technology (FUOYE**JET**), **9(4)**, 693-698. https://dx.doi.org/10.4314/fuoyejet.v9i4.19

http://.doi.org/10.46792/fuoyejet.v9i4.C

that by providing quantifiable information regarding the development of corrosion as aggressive circumstances arise in the concrete as a result of chloride ingress or carbonation, corrosion monitoring can play a critical role in scheduled maintenance and life prediction [Kioumarsi, *et al.*, (2019), Malaret, (2022)]. Additionally, HCl has been used extensively as corrosion medium by [Nikitasari, et al., (2022), Fernandez, et al.,(2016), Patil, *et al.*, (2022)].

This research therefore tends to compare the corrosion properties (corrosion rates) obtained from weightloss approach and the potentio-dynamic polarization resistance on embedded steel in a reinforced concrete beam at different levels of concentration of environment.

2 THEORETICAL ANALYSES

2.1 ARRHENIUS EXPRESSION ON CORROSION

Using the new Arrhenius expression and the generalized reaction depicted in equation 1

$M \rightleftharpoons M^{z+} + ze$ (1)

where M is a metal that forms M^{z+} ions in solution, we can now derive an equation describing corrosion kinetics.

Consider the rate of the anodic (oxidation, corrosion) reaction, ka (equation 2)

$ka = ka' exp(\frac{-\Delta G0}{RT})$ (2)

The reaction entails the liberation of electrons, and its advancement may be quantified as a current density, i (current per unit area). The exchange current density, i0, is defined as the current per unit area flowing in both directions when an electrode reaction is at equilibrium, corresponding to its equilibrium potential. If i0 is minimal, then negligible current flows, and the responses in dynamic equilibrium are often sluggish. Similarly, a high i0 results in a rapid reaction. The metal influences the value of i0, regardless of whether the reaction directly involves the metal, as seen in equation 3.$i_0 = zFka = zFk'_a exp(\frac{-\Delta G^0}{RT})$ (3)

If overpotential is applied, the activation energy is changed equation 4 shows the result of the change

$i_a = i_0\ exp(\frac{\alpha zF\eta}{RT})$ (4)

This represents a variant of the Tafel equation. The Tafel equation can be expressed in several equivalent forms. The expression 2.303RT/αzF is denoted as βa and is referred to as the anodic Tafel slope. It possesses units of volts per decade of current. In a similar manner, if the cathodic reaction is examined, the number would be −2.303RT(1−α)zF, as (1 − α) is relevant instead of α, and E - Ee is negative. The specified amount is the cathodic Tafel slope, denoted as βc.

The standard representation of Tafel's equation is expressed as equation 5.

$\boldsymbol{\eta} = a + \mathrm{b_a}\ log\ \mathrm{i_a}$ (5)

$where\ a = \frac{-2.303RT}{azF} log\ i_0$

By analysing the reaction as both a chemical and electrical process and employing algebraic manipulation, we have shown that the applied potential is proportional to the logarithm of the resultant corrosion current. This is distinctly unlike to Ohmic behaviour, where the applied potential is precisely proportionate to the resultant current.

2.2 GRAVIMETRIC/WEIGHT LOSS EXPRESSION

The gravimetric method involves immersing a metal sample in a corrosive environment and measuring the weight loss over time. The corrosion rate (CR) can be calculated using the equation 6.

$CR = (KW\_loss)/\rho AT$ (6)

Where:

(K) is a constant=87.6

(W_loss)is the weight loss in grams.

(ϱ) is the density of the steel sample

(A) is the total surface area of the coupon in square centimeters.

(t) is the exposure time.

Potentio-dynamic polarization provides information about localized corrosion behavior (e.g., pitting), while the gravimetric method gives an overall corrosion rate.

3 EXPERIMENTAL PROCEDURES

3.1. CONCRETE CONSTRITUENTS

The concrete specimens were made using Type I Portland cement, which is widely used in Nigeria. Crushed limestone that had been processed from nearby quarries served as the coarse aggregate for this investigation. According to ASTM Standard C-127 (2003), the coarse aggregates' average specific gravity and absorption were found to be 2.5 and 1.3%, respectively. The fine aggregate utilized was medium coarse sand. The fine aggregates had a specific gravity of 2.6 and an absorption of 0.40%, respectively. Concrete was mixed and allowed to cure in potable water serving as control, 0.1 M, 0.2 M and 0.3 M of Hydrochloric acid solution (HCl). The steel specimen (figure 1) is 16mm diameter with and 100mm length embedded in 1:2:4 concrete mixes up to 60mm depth having external protrusion of 40mm for contact with the electrodes of potentio-dynamic setup (figures 2a and b) and similar samples with no protrusion for weight loss experiment. These experiments were carried out three times to validate and correlate the results obtained at initial trial.

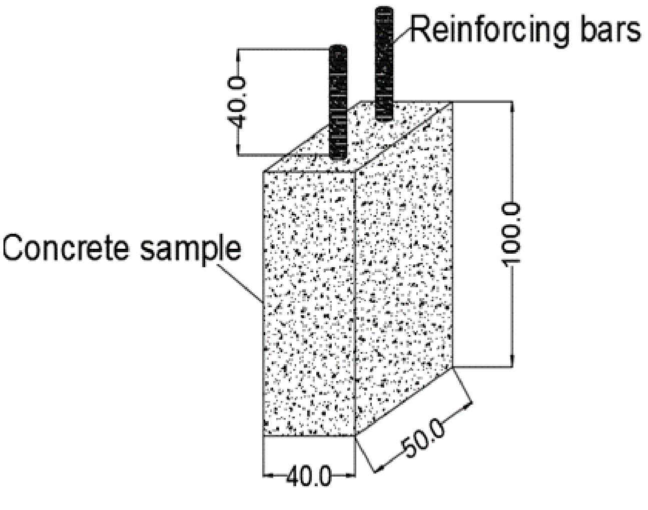

http://dx.doi.org/10.46792/fuoyejet.v9i4.19

Figure 1: Illustration of concrete samples with embedded steel

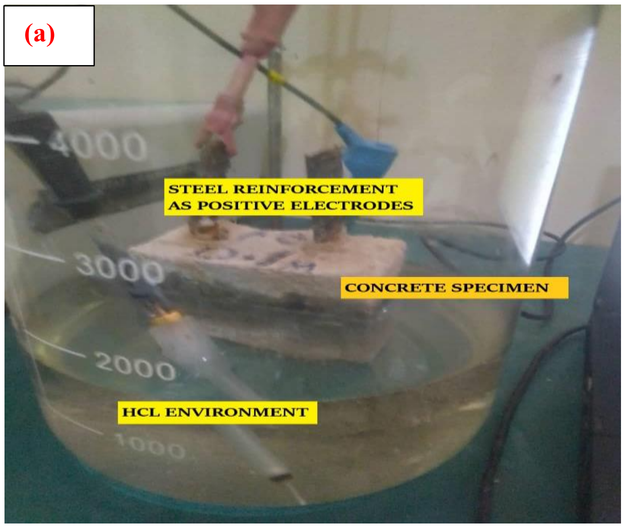

Figure 2: (a) Illustration of concrete samples with embedded steel

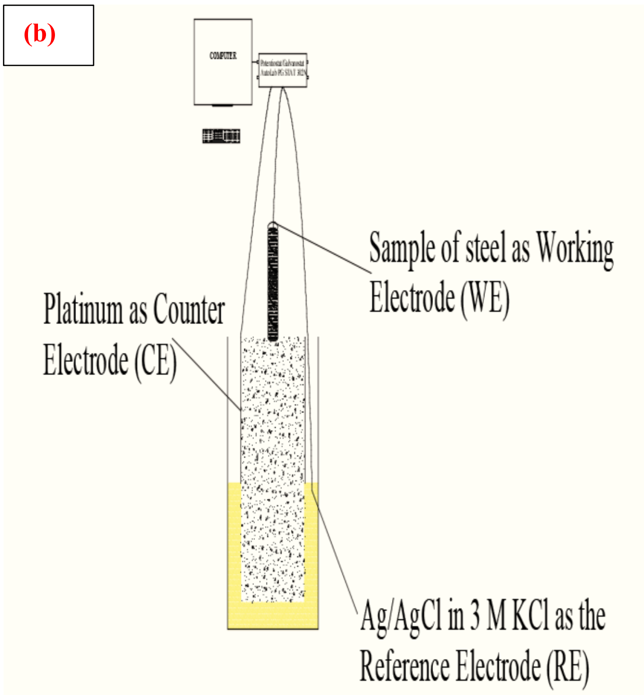

Figures 2:(b) Experimental setup for PDP (b) Schematic diagram of PDP setup.

3.3. PREPARATION OF WEIGHT LOSS METHOD

The experiment was conducted to precisely and correctly calculate the specimen's weight loss as a result of corrosion in accordance to [ASTM, G1-03 (2003) and ASTM, C-127 (2003)]. Prior to any further processing, the steel specimens having composition of high yield properties, length of 100mm and diameter of 16mm were cleaned and polished using sandpaper, tissue paper, and a clean cloth. To degrease them, they were first cleaned with tap water, then with distilled water and lastly with acetone. Following a thorough air-drying process, the specimens were weighed to four decimal places on an analytical balance. The objects' weights were recorded and a cast concrete sample of 140mm x 50mm x 40 mm was utilized. After that, the samples of reinforced concrete were left to cure for seven, fourteen, twenty-one, and thirty-eight days in various hydrochloric acid concentration media (0.1 M, 0.2 M, 0.3 M, and 0.0 M). The corrosion rate was determined using Equation 5.

4 RESULTS AND DISCUSSION

4.1: Results of Weightloss Method

The results obtained for various concentration levels are illustrated in Table 1. It indicates gradual reduction in the corrosion rates as the curing ages increase. The corrosion rate for 7days, 14days, 21 days and 28 days for 0.0 M are 0.0367 mmpy 0.0146mmpy, 0.0122mmpy, 0.0073mmpy while 0.1 M, are 0.0367mmpy, 0.0165mmpy, 0.0122mmpy and 0.0100mmpy respectively . Also, the corrosion rates for 0.2 M for the respective curing ages are 0.0403mmpy, 0.0165mmpy,0.0110mmpy and 0.0073mmpy and 0.3 M of HCl are 0.0367mmpy, 0.0146mmpy, 0.0122mmpy and 0.0073mmpy. This is further illustrated in figure 2.

Table 1: Weightloss method results

Acidic content	*Corrosion rate (mmpy)*			
	Curing ages			
	7	**14**	**21**	**28**
0.1 M	0.0367	0.0165	0.0122	0.0100
0.2 M	0.0330	0.0091	0.0097	0.0082
0.3 M	0.0403	0.0165	0.0110	0.0073
0.0 M	0.0367	0.0146	0.0122	0.0073

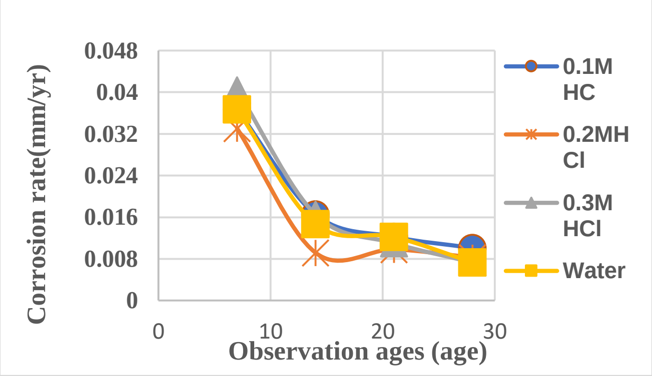

Figure 2: Weightloss results of corrosion rates

4.2. Potentio-dynamic Polarization Results

The PDP experiments being an electrochemical approach provides further description of the corrosion mechanism of the steel. The results (table 2) showed a comparative insight to the corrosion rates of the steel specimen embedded in the concrete. It was revealed that corrosion rates for 0.0 M of HCl are 0.117mmpy, 0.110mmpy, 0.0989mmpy and 0.0591. 0.1 M of acid at 7days, 14days, mmpy 21 days and 28days are 0.0853mmpy, 0.0742mmpy, 0.0657mmpy and 0.0578mmpy. In addition, corrosion rates for 0.2 M for each curing ages are 0.0804mmpy, 0.074mmpy, 0.07743mmpy and 0.0683mmpy while for 0.3 M, the results are 0.153mmpy,

http://dx.doi.org/10.46792/fuoyejet.v9i4.19

0.1084mmpy,0.07192mmpy and 0.0620mmpy. This is further illustrated in figure 3.

Table 2: Potentio-dynamic Polarization results

Acidic content	*Corrosion rates (mmpy)*			
	Curing ages (days)			
	7	**14**	**21**	**28**
0.1 M	0.0853	0.0742	0.0657	0.0578
0.2 M	0.0804	0.074	0.07743	0.0683
0.3 M	0.153	0.1084	0.07192	0.0620
0.0 M	0.117	0.110	0.0989	0.0591

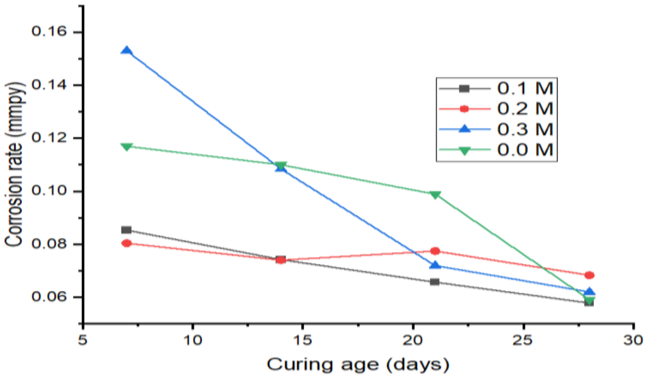

Figure 3: Graph of Potentio-dynamic polarization results

4.3 Tafel Plots of Potentio-dynamic Polarization (PDP)

Tafel extrapolation is a popular polarization method for measuring corrosion rates since it is a faster experimental approach than the traditional weight-loss estimation method (Kakaei *et al.,* 2019). The Tafel equation, which explains the connection between electrode potential and current density, is shown graphically by Tafel charts. They are employed to keep an eye on how quickly concrete's reinforcing steel corrodes. The figures indicate that reaction kinetics are largely constant throughout time, with a steeper slope at lower potentials and a more gradual slope at higher potentials. Tafel plots aid in tracking changes in electrochemical behaviour over time in the setting of concrete degradation. The graphs demonstrate a steady rise in current density over time at a given potential, which is indicative of a cathodic response that lowers the rate of corrosion. Tafel plots of HCl at 0.2M concentration level are displayed in Figure 5, which generally illustrates a trend of declining potential with rising current density logarithms. This is because more metal ions are oxidised at the anode and more hydrogen ions are reduced at the cathode when the current density rises. This results in a drop in potential as more electrons are moved from the metal to the solution.

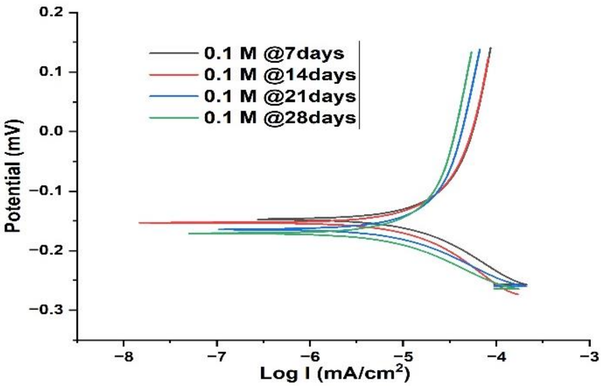

Figure 4: TAFEL Plot of 0.1M HCl concentration level

Tafel plots are a helpful tool for researching the corrosion behaviour and potentials of metals, to sum up. They can be used to analyse corrosion rates in a variety of applications and offer a visual representation of the relationship between electrode potential, current density, and potential. Tafel plot of HCl at 0.2M concentration level is displayed in Figure 5, which generally illustrates a trend of declining potential with rising current density logarithms. This is because more metal ions are oxidized at the anode and more hydrogen ions are reduced at the cathode when the current density rises. This results in a drop in potential as more electrons are moved from the metal to the solution.

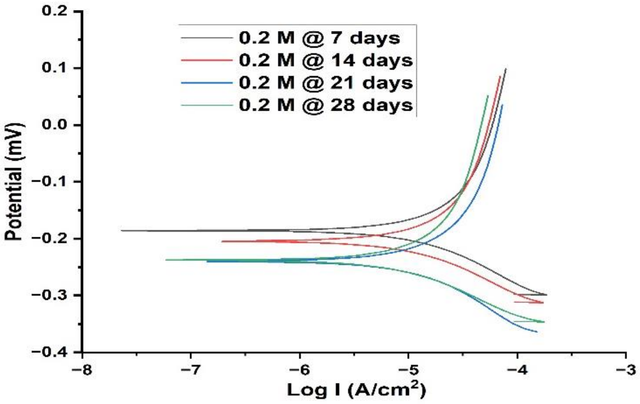

Figure 5: TAFEL Plot of 0.2M HCl concentration level

They Tafel plots are employed to keep an eye on how quickly concrete's reinforcing steel corrodes. At lower potentials, the plots exhibit a steep slope, while at higher potentials, a more gradual slope. Tafel plots analyze the places where the reduction and oxidation reactions converge to provide the corrosion current and potential in the context of concrete corrosion. The graphs demonstrate a steady rise in current density over time at a given potential, which is indicative of a cathodic response that lowers the rate of corrosion. More metal ions being oxidised at the anode and more hydrogen ions being reduced at the cathode cause the general trend of decreasing potential with increased current density.

http://dx.doi.org/10.46792/fuoyejet.v9i4.19

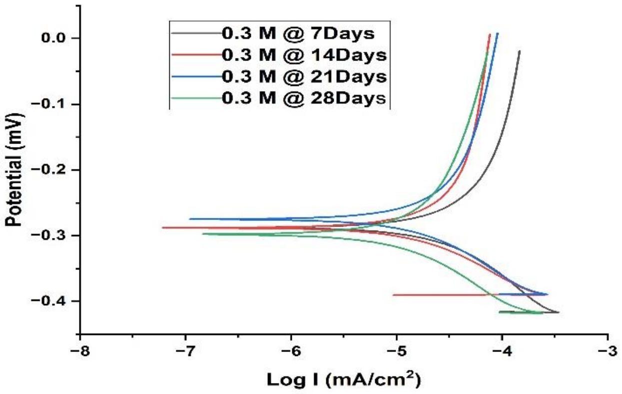

Figure 6: TAFEL Plot of 0.3M HCl concentration level

The Tafel equation, which explains the connection between electrode potential and current density, is shown graphically by Tafel charts. They are employed to keep an eye on how quickly concrete's reinforcing steel corrodes. At lower potentials, the plots exhibit a steep slope, while at higher potentials, a more gradual slope. Tafel plots analyse the places where the reduction and oxidation reactions converge to provide the corrosion current and potential in the context of concrete corrosion. The graphs demonstrate a steady rise in current density over time at a given potential, which is indicative of a cathodic response that lowers the rate of corrosion. More metal ions being oxidised at the anode and more hydrogen ions being reduced at the cathode cause the general trend of decreasing potential with increased current density

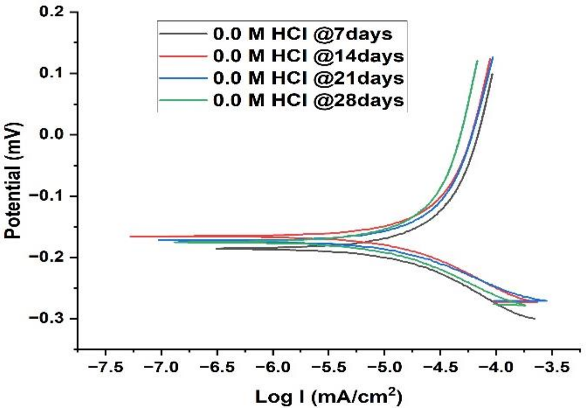

Figure 7: TAFEL Plot of 0.0M HCl concentration level

The graph shows the corrosion rate in millimeters per year, while the cure age is represented in days. The graph consists of four lines, each representing a distinct corrosion property at different curing ages. The color coding of these lines is blue for water at 7days, red for water at 14days, grey for water at 21days and purple for water at 28days. The potential varies with different current density. The reaction is a cathodic reaction by virtue of the direction of the graph hence the decrease in corrosion rates observed. The material becomes increasingly resistant to corrosion over time, as the rate decreases as the curing age increases. This can change depending on the concentration or if water alone is present. As the curing age increases, the corrosion rate decreases, indicating that the concrete's resistance to corrosion increases as it cures.

Table 3: Summary table of Potentio-Dynamic Polarization Resistance Test

ACID ENVIRONMENT HCl	Concentration (M)	Curing Age (days)	E_{corr} (V)	i_{corr} (A/cm²)	Polarization Resistance	Slope of Tafel Plot β_a (V/dec)	Slope of Tafel Plot β_c (V/dec)
	0.1	7	-0.148	7.34×10^{-6}	2166.6	0.088	0.063
		14	-0.153	6.38×10^{-6}	2544.1	0.089	0.065
		21	-0.165	5.66×10^{-6}	2599.8	0.089	0.055
		28	-0.171	4.97×10^{-6}	3020.0	0.094	0.055
	0.2	7	-0.186	6.92×10^{-6}	2446.0	0.099	0.067
		14	-0.204	6.37×10^{-6}	2661.7	0.096	0.066
		21	-0.240	6.66×10^{-6}	2849.8	0.104	0.075
		28	-0.238	5.88×10^{-6}	3267.4	0.120	0.070
	0.3	7	-0.288	1.32×10^{-6}	1326.7	0.097	0.069
		14	-0.289	9.33×10^{-6}	1142.7	0.105	0.061
		21	-0.299	6.19×10^{-6}	2857.0	0.106	0.066
		28	-0.299	5.33×10^{-6}	2862.1	0.089	0.058
	0.0	7	-0.186	1.01×10^{-5}	2110.9	0.121	0.082
		14	-0.166	9.42×10^{-6}	2098.3	0.113	0.017
		21	-0.172	8.51×10^{-6}	2019.0	0.103	0.064
		28	-0.175	5.08×10^{-6}	2604.1	0.068	0.055

5 CONCLUSION

. Based on the results obtained from the research, the following conclusion were drawn:

i. Weight loss method even though old is still valid as an alternative way of comparing or correlating the results of corrosion determination.
ii. The results obtained from the two methods exhibited closeness and parity especially in downward trends of corrosion rate.
iii. Potentio-dynamic polarization method provided a detailed explanation and direction about the kinetics of the corrosion process in this research.
iv. Cathodic reactivity was more pronounced when 0.3 M of HCl was utilized, this is as a result of free/more hydrogen ions in the solution.

ACKNOWLEDGMENT

The authors wish to appreciate the technologists in all the laboratories where the research was conduction both in Covenant University, Ota Ogun State and the Federal Polytechnic, Ado Ekiti, Ekiti state.

REFERENCES

Cáceres, A., Casales, M., & Martínez, L. (2019). A comparative study of gravimetric and electrochemical techniques for the evaluation of corrosion inhibitor activity onset and efficiency in pipeline CO_2 environments. Ingeniare, 27(4), 625–634. https://doi.org/10.4067/S0718-33052019000400625

Kakaei, K., Esrafili, M. D., & Ehsani, A. (2019). Graphene and Anticorrosive Properties Interface Science and Technology, 27, 303–337. https://doi.org/10.1016/B978-0-12-814523-4.00008

Song, H. W., & Saraswathy, V. (2007). Corrosion monitoring of reinforced concrete structures - A review. International Journal of Electrochemical Science, 2(1), 1–28. https://doi.org/10.1016/s1452-3981(23)17049-0

Zhang, X. L., Jiang, Z. H., Yao, Z. P., Song, Y., & Wu, Z. D. (2009). Effects of scan rate on the potentiodynamic polarization curve obtained to determine the Tafel slopes and corrosion current density. Corrosion science, 51(3), 581-587.

Kumar, V., Singh, R., and Quraishi, M. A. (2013). A study on corrosion of reinforcement in concrete and effect of inhibitor on service life of RCC. Journal of Materials and Environmental Science, 4(5), 726–731.

Al-Saidy, A. H., Al-Harthy, A. S., and Al-Jabri, K. S. (2009).

http://dx.doi.org/10.46792/fuoyejet.v9i4.19

Effect of damaged concrete cover on the structural performance of CFRP strengthened corroded concrete beams. Concrete Repair, Rehabilitation and Retrofitting II - Proceedings of the 2nd International Conference on Concrete Repair, Rehabilitation and Retrofitting, ICCRRR, November 2014, 437–438.

ASTM Standard G1-03 (2003): "Standard Practice for Preparing, Cleaning and Evaluating Corrosion Test Specimens." ASTM International, pp. 15-21

ASTM Standard C-127 (2003); *Standard Test Method for Density, Relative Density (Specific Gravity), and Absorption of Coarse Aggregate 1*. 1–7

Usman, A. D., Victoria, A. F., & Okoro, L. N. (2016). Weight Loss Corrosion Study of Some Metals in Acid Medium. Journal of Advances in Chemistry, 11(2), 3434–3440. https://doi.org/10.24297/jac.v11i2.2211

Tachibana, Y., Maeda, K.-I., Kajikawa, Y., & Kawamura, M. (1990). Mechanical behavior of RC beams damaged by corrosion of reinforcement. Elsevier Applied Science, 178–187.

Sistonen, E., Cwirzen, A., and Puttonen, J. (2008): "Corrosion Mechanism of Hot-Dip Galvanised Reinforcement Bar in Cracked Concrete." Corrosion Science, Vol. 50(12), pp. 3416–3428.

Nikitasari, A., Priyotomo, G., Royani, A., Sundjono, S. (2022). 'Exploration of Eucheuma Seaweed Algae Extract as a Novel Green Corrosion Inhibitor for API 5L Carbon Steel in Hydrochlorid Acid Medium', International Journal of Engineering, 35(3), pp. 596-603. doi: 10.5829/ije.2022.35.03C.13

Malaret, F. (2022). Exact calculation of corrosion rates by the weight-loss method. Experimental Results, 3, 1 12. https://doi.org/10.1017/exp.2022.5 Fernandez, I., Bairán J. M., and Marí A. R. (2015): "Corrosion Effects on the Mechanical Properties of Reinforcing Steel Bars.

Fernandez, I., Bairán J. M., and Marí A. R. (2015): "Corrosion Effects on the Mechanical Properties of Reinforcing Steel Bars Fatigue and σ–ε Behavior." Construction and Building Materials, Vol. 101(2015), pp. 772–783.

Fernandez, I., Herrador, M. F., Marí A. R., and Bairán J. M. (2016): "Structural Effects of Steel Reinforcement Corrosion on Statically Indeterminate Reinforced Concrete Members." Materials and Structures, Published online

Kioumarsi, M., Baghban, M. H., & Imperatore, S. (2019). Effect of time dependent corrosion rate on residual capacity of corroded RC beam. IOP Conference Series: Materials Science and Engineering, 652(1). https://doi.org/10.1088/1757-899X/652/1/012031

Malaret, F. (2022). Exact calculation of corrosion rates by the weight-loss method. Experimental Results, 3, 1 12. https://doi.org/10.1017/exp.2022.

Khavasfar, A., Moayed, M.H., Jafari, A.H. (2007) "An Investigation on The Performance of an Imidazoline Based Commercial Corrosion Inhibitor on CO_2 Corrosion of Mild Steel" International Journal of Engineering, Transactions A: Basics, Vol. 20, No. 1, (2007), 35-44.

Patil, V. G., Somasundaram, B., Kandaiah, S., Ramesh, M. R., & Kumar, S. (2022). High Temperature Corrosion Behavior of High Velocity Oxy Fuel Sprayed NiCrMoFeCoAl-30%SiO_2 and NiCrMoFeCoAl-30%Cr_2O_3 Composite Coatings on ASTM SA213-T22 Steel in a Coal-fired Boiler Environment. *International Journal of Engineering, Transactions A: Basics*, *35*(7), 1416–1427. https://doi.org/10.5829/ije.2022.35.07a.19

http://dx.doi.org/10.46792/fuoyejet.v9i4.19